Mechanical Loading Prevents Obesity-Associated Bone Loss by Maintaining the Balance between Adipocytes and Osteoblasts

Xinle Li
Tianjin Medical University
Jie Li
Tianjin Medical University
Daquan Liu
Tianjin Medical University
Keyu Wang
Tianjin Medical University
Hiroki Yokota
Indiana university-Purdue University Indianapolis
Ping Zhang (pizhang@tmu.edu.cn)
Department of Anatomy and Histology, School of Basic Medical Sciences, Tianjin Medical University
https://orcid.org/0000-0002-6336-6611

Research

Keywords: Adipocytes, Osteoblasts, Obesity, Bone loss, Knee loading

Posted Date: July 29th, 2020

DOI: https://doi.org/10.21203/rs.3.rs-49548/v1

Abstract

Background: Globally increasing obesity is closely linked to bone homeostasis. Maintaining the balance between differentiate of adipocytes and osteoblasts from bone marrow mesenchymal stem cells (BMSCs) is important for bone homeostasis. While mechanical loading has been shown to improve bone remodeling by promoting osteoblast differentiation, little is known about its effects on obesity-associated bone loss.

Methods: Using obese mice induced by high-fat diet and ovariectomy (OVX), the effects of mechanical loading in a form of knee loading (1 N, 5 Hz, 6 min/day) was applied with for 4 weeks. The mice were sorted into five groups: standard diet control (SC), high-fat diet control (HF), HF and loading (HFL), HF and ovariectomy (HO), and HO and loading (HOL). Femurs were harvested for histomorphometry analysis. Bone marrow-derived cells were isolated to examine the banlance between differentiation of adipocytes and osteoblasts. Immunohistochemical analyses and Western blotting analyses were performed to evaluate markers for adipocytes, osteoblasts, and Wnt signaling.

Results: High-fat diet presented higher body weight, body fat, and body mass index (BMI), as well as bone loss than standard diet, and the detrimental changes in OVX mice were even higher. The daily application of knee loading significantly decreased BMI, the numbers and perimeter of adipocytes, and the differentiation of adipocytes. The expression of C/EBPα and PPARγ were suppressed by knee loading. The loaded group also presented a significant increase in bone mineral density and contents, and the circumference of trabecular bone. Regarding osteoblasts, knee loading enhanced the number of osteoblasts on bone surface, differentiation of osteoblasts, and the level of Runx2 and ALP. Furthermore, Wnt signaling involved in the effect of knee loading on attenuating obesity-induced bone loss.

Conclusions: This study supported evidence that knee loading offers a new therapeutic option to prevent obesity-related bone loss by altering the balance between adipocytes and osteoblasts in the bone marrow, and the effect is associated with Wnt signaling.

Background

Obesity and its associated metabolic sequela are increasing globally [1], whereas the relationship between adiposity and bone homeostasis is not well understood [2]. The bone marrow represents an important compartment to regulate mineral homeostasis [3]. Adipose tissue in the bone marrow (marrow adipose tissue; MAT) plays a critical role in obesity [4]. Adipocytes are generated from mesenchymal stem cells (MSCs) in bone marrow milieu, and are derived from the same stem cell lineage as osteoblasts [5, 6]. It is reported that dysregulated differentiation of MSCs is likely to contribute to inducing osteoporosis [7]. Adipocyte differentiation from MSCs is triggered by the activation of CCAAT/enhancer-binding protein β (C/EBPβ) and peroxisome proliferator-activated receptor γ (PPARγ) [8]. By contrast, osteogenesis is mainly regulated by runt-related transcription factor 2 (Runx2) as a cell-specific member of the Runt family, as the master regulator to control osteoblast differentiation [9]. We rationalized that an

increase of adipose tissues with obesity-linked bone loss can potentially be associated with an imbalance of cell fates in the bone marrow between osteoblasts and adipocytes. Therefore, regulating their differentiation might be a therapeutic option to suppress obesity-associated bone loss.

Bone is a dynamic tissue, which is sensitive to the mechanical environment [10], and a group of joint loading modalities, applied to synovial joints such as the elbow, knee, and ankle, has been developed to evaluate bone's responses to mechanical loading [11–16]. Previous studies have shown that knee loading not only stimulates wound healing and bone formation of the femur but also prevents bone loss associated with necrotic and osteoporotic femora [17–19]. Knee loading is also reported to inhibit obesity-associated hepatic steatosis [20], but its effect on obesity-associated bone loss has not been elucidated.

A Wnt signaling pathway is known to be activated by mechanical loading for inducing bone formation [21], and it also plays a pivotal role in bone remodeling and regeneration [22–24]. Studies demonstrated that Wnt signaling inhibited adipocyte differentiation by blocking transcription factors such as CCAAT/enhancer-binding protein α (C/EBPα), and peroxisome proliferator-activated receptor γ (PPARγ) [25–27]. A Runx/Cbfβ complex promotes Wnt10b/β-catenin signaling and regulates the osteoblast-adipocyte lineage [28]. We have shown that Wnt3a is involved in loading-driven bone formation and can potentially serve as a therapeutic target for osteoporosis [29]. However, little is known about the role of loading-driven Wnt/β-catenin signaling in the balance of cell fates towards osteoblasts and adipocytes in the pathogenesis of obesity-linked bone loss.

We hypothesized herein that mechanical loading can significantly alter the osteoblast-adipocyte lineage and reduce obesity-linked bone loss. To test the hypothesis, we induced obese mice by a high-fat diet (HFD) and/or ovariectomy (OVX) and examined the effects of knee loading on bone homeostasis in obese mice. Bone marrow-derived cells were isolated to evaluate the differentiation of adipocytes and osteoblasts. The changes in the levels of adipogenic and osteogenic genes were determined to evaluate the effects of knee loading on the proliferation and differentiation of MSCs. BMD, BMC and morphology of the femurs were assessed by X-ray imaging and histology, and femurs were harvested for Western blotting to evaluate the role of Wnt/β-catenin signaling.

Materials And Methods

Animals and materials preparation

Fourteen-week-old C57BL/6 female mice (~ 18 g, Animal Center of Academy of Military Medical Sciences, China) were employed. The animals were housed in a temperature-controlled room (22–25 °C, 50–60% humidity) on a dark-light cycle of 12:12-h under pathogen-free conditions. They were handled by a professional person and had access to water and food. All experiments were carried out in accordance with the National Institutes of Health Guide for Care and Use of Laboratory Animals and were approved by the Ethics Committee of Tianjin Medical University. We acquired minimum essential medium alpha

(MEM-α), fetal bovine serum (FBS), penicillin, streptomycin, and trypsin from Invitrogen (Carlsbad, CA, USA), while other agents were obtained from Sigma (St. Louis, MO, USA) unless otherwise stated.

Experimental design

After 1 week of acclimation, one hundred and ten mice were randomly sorted into five groups: the control group fed with a standard chow diet (SC; *N* = 22), high-fat diet group (HF; *N* = 22, D12492, Beijing Huafu Kang Biological Co. Beijing, China), high-fat diet and knee loading group (HFL; *N* = 22), high-fat diet in combination with ovariectomy (OVX) group (HO; *N* = 22), and high-fat diet in combination with OVX and knee loading group (HOL; *N* = 22). Two OVX groups (HO and HOL) underwent bilateral ovariectomy, while three pseudo-OVX groups (SC, HF, and HFL) underwent sham surgery. In addition to SC, the other four groups received a high-fat diet. After 4 weeks, two groups (HFL and HOL) received knee loading for the next 4 weeks (Fig. 1a).

Ovariectomy

Mice were anesthetized using 1.5% isoflurane (IsoFlo; Abbott Laboratories, North Chicago, IL, USA). We used a scalpel to make an incision on the dorsal skin of the midline, and removed the ovaries with scissors (Fig. 1b). For mice undergoing pseudo-OVX surgery, the same procedure was conducted without isolating the ovaries. To alleviate the surgery-linked pain, mice received 0.05 mg/kg buprenorphine hydrochloride every 8 h during the first 3 days. Also, 1% pramoxine hydrochloride ointment was applied daily at the incision site [19,29].

Mechanical loading

After 4 weeks of high-fat diet and OVX, mice in HFL and HOL groups were mask-anesthetized using 1.5% isoflurane and loaded onto both knees in the lateral-medial direction using a custom mechanical loader. Daily dynamic loads (1 N at 5 Hz) were applied every day to each of the right knees and then the left knee for 3 minutes (loading total time was 6 min/day), for 4 weeks (Fig. 1c). The lateral and medial sides of the femur and tibia were in contact with the loading rod and the stator, respectively (Fig. 1d). The sham-treated control mice (SC) and obese mice (HF and HO) were given sham loading, in which mice were placed on the loading table and anesthetized, but did not receive any loads.

Body weight and body fat composition analysis

We measured the body weight and food intake weekly and daily, respectively, by a blinded person. Body fat content and body mass index were determined by a systemic composition analyzer (ImpediVet, Pinkenba, Qld, Australia) [20].

Histology, MacNeal's and immunohistochemistry assays

We harvested femurs fixed them using 10% neutral buffered formalin. The samples were decalcified in 10% ethylenediaminetetraacetic acid (EDTA, PH = 7.4) for 3 weeks, and embedded in paraffin after dehydration. We prepared 5-μm thick sections along the coronal plane using a Leica RM2255 microtome (Leica Microsystems Inc., Bannockburn, IL). Using H&E stained femoral sections, we determined A.ar/T.ar (in %, T.ar = total tissue area, and A.ar = adipocytes area), adipocyte perimeter, adipocyte number [30] and B.ar/T.ar (in %, T.ar = total tissue area, and B.ar = trabecular bone area), as well as bone trabecular circumference in the 1.9 mm^2 sample area of the proximal femoral growth plate[31]. Furthermore, MacNeal's stained sections were used to determine the osteoblast number on the trabecular bone surface (osteoblasts number/bone surface, N.Ob/BS/mm) [32].

The expression of Wnt3a was analyzed by immunohistochemistry. After deparaffinization and rehydration, the distal femur sections were incubated with primary antibodies and an immunohistochemical color reaction was performed using a 3, 3'-diaminobenzidine substrate kit and hematoxylin as a counterstain. One of every 10 slices (5 slices in total) was chosen for quantification in a blinded fashion. We determined the ratio of positively stained cells in 10 fields at 200× magnification per section [14].

Isolation of bone marrow mesenchymal stem cells and their culture

After sacrifice, the femur and tibia were washed with MEM-α (Thermo Fisher Scientific) for collecting BMSCs. The cells were isolated by centrifugation using a Ficoll low-density gradient and cultured in MEM-α containing 10% FBS [33].

Adipogenic differentiation assay and oil-red O staining

For adipogenic differentiation, bone marrow-derived cells (2×10^6 cells/ml in 6-well plates) were cultured for 72 h in adipogenic medium (MEM-α containing 10% FBS), with 0.5 μM dexamethasone, 0.25 mM methylisobutylxanthine, 5 μg/ml insulin, and 50 μM indomethacin, and then treated for an additional 48 h with 5 μg/mL insulin.

Differentiated adipocytes were fixed in 4% paraformaldehyde and stained in a 60% saturated oil red O solution. For quantification, isopropanol was employed to extract oil red O and optical absorbance at 520 nm was measured [27].

Measurements of bone mineral density and bone mineral content in vivo

Mice were anesthetized by 1.5% isoflurane to maintain in the prone position, and measurements were performed in about 5 min per mouse. In the femur, we determined bone mineral density (BMD, g/cm^2) and bone mineral content (BMC, g) using peripheral dual-energy X-ray absorptiometry (pDEXA; PIXImus II; Lunar, Madison, WI, USA) [19].

Osteoblast differentiation assay and ALP staining

For osteoblast differentiation, bone marrow-derived cells (2×10^6 cells/ml) were cultured in osteogenic differentiation medium (MEM-α containing 10% FBS, 10 nM dexamethasone, 50 μg/ml ascorbic acid, and 10 mM β-glycerophosphate). The medium was changed every 2 days, and cells were cultured for 14 days [29].

We performed alkaline phosphatase (ALP) staining (Sigma). We fixed cells in citrate-buffered acetone, incubated in the alkaline-dye mix, and counterstained with Mayer's Hematoxylin. Five fields (400×) were randomly selected in each well, and the ratio of the number of ALP-positive cells to that of total cells was determined.

Western blotting analysis

After sacrifice, the femurs were removed. Protein samples were isolated from the femurs using a mortar and pestle and lysed in a radioimmunoprecipitation assay lysis buffer with protease inhibitors and phosphatase inhibitors (Roche Diagnostics GmbH, Mannheim, Germany). The isolated proteins were electro-separated and transferred to a polyvinylidene difluoride membrane (Millipore, Billerica, MA, USA). Primary antibodies specific to Wnt3a (Abcam, Cambridge, MA, USA), β-catenin, LRP5, Runt-related transcription factor 2 (Runx2), PPARγ, C/EBPα (Cell Signaling, Danvers, MA, USA), ALP (Proteintech, Wuhan, China) and β-actin (Sigma, St Louis, USA) were employed. After incubation with horseradish peroxidase-conjugated secondary antibodies, chemiluminescence signals were detected and processed with reference to β-actin [27].

Statistical analysis

We expressed data as mean ± standard error of mean (SEM). For comparisons among more than 2 groups, we employed one-way analysis of variance (one-way ANOVA) and a post-hoc test of least significant difference (LSD) using SPSS software (version 20.0). We also conducted correlation analysis using Pearson correlation coefficients. The relative parameters (% change) such as body weight, body fat content, BMD, and BMC were calculated as ((S-B)/B × 100 in %, where S= "sacrifice" and B = "baseline"). All comparisons were two-tailed and we assumed statistical significance at $P < 0.05$. The asterisks (*, ** and ***) represent $P < 0.05$, $P < 0.01$, and $P < 0.001$, respectively. The pound signs ($^{\#}$, $^{\#\#}$ and $^{\#\#\#}$) represent $P < 0.05$, $P < 0.01$, and $P < 0.001$, respectively.

Results

All animals tolerated the procedures, and no bruising or tissue damage was detected at the surgical and loading site. Because of OVX, the uterine mass was 91% lower in HO than HF. However, HFL's uterine mass was not altered from that in HF (Fig. 1e).

Knee loading reduced body weight and fat in obese mice

The body weight among the five groups showed significant variations (Fig. 2a). In response to the high-fat diet, the HF animals were 50% heavier than in the SC group ($P < 0.001$), and the HO group animals were 14% heavier than in the HF group ($P < 0.05$). Regarding the rate of weight change, the HO group also showed more weight change than the HF animals ($P < 0.05$). After loading, body weight was reduced in both HF and HO groups (both $P < 0.001$; Fig. 2b and c).

The change in body fat content followed the same trend to body weight. HF had 98% higher body fat content than SC ($P < 0.001$), and HO had 66% higher than HF ($P < 0.001$). Knee-loading decreased body fat content in the HFL group (72% decrease) and the HOL group (66% decrease), compared to that in the HF and HO groups, respectively (both $P < 0.001$; Fig. 2d and e).

Regarding BMI, both the HF and HO groups had a larger BMI than the SC and HF groups, respectively ($P < 0.001$ in HF; $P < .05$ in HO). The HFL and HOL groups also presented a significant decrease in BMI compared to HF and HO groups (both $P < 0.001$; Fig. 2f). Interestingly, there was no significant difference in food intake among all groups ($P > 0.05$; Fig. 2g).

Knee loading inhibited adipogenic differentiation of BMSCs

To determine the loading-driven changes of bone marrow adipocytes, the number, perimeter, and A.ar/T.ar were evaluated using H&E-stained femurs (Fig. 3a). HF and HO presented a significant increase in bone marrow adipocytes (number, perimeter, and A.ar/T.ar), compared to the SC ($P < 0.05$, $P < 0.01$, $P < 0.01$ respectively) and HF group (all $P < 0.001$). The two groups with knee-loading (HFL and HOL) exhibited reduced numbers, perimeter, and A.ar/T.ar of bone marrow adipocytes, compared to the non-loaded counterparts (HF and HO), respectively ($P < 0.05$ in HFL; $P < 0.001$ in HOL; Fig. 3c-e).

Oil-red O staining was used to detect adipocyte differentiation from bone marrow cells (Fig. 3b). Compared to SC and HF, HF and HO led to a significant increase in the number of differentiated adipocytes and OD520, respectively (both $P < 0.001$). However, the two loaded groups (HFL and HOL) suppressed the number of oil red O-positive adipocytes and OD520 compared to the non-loaded groups (HF and HO) (both $P < 0.001$; Fig. 3f).

We examined the expression levels of C/EBPα and PPARγ to evaluate adipocyte differentiation (Fig. 3g). Their levels in HF and HO were significantly higher than those in SC and HF, respectively (all $P < 0.001$).

After knee-loading, these levels were reduced (both $P < 0.01$ in HFL; both $P < 0.001$ in HOL; Fig. 3h and i).

Knee loading induced bone loss reduction in obese mice

Compared to animals in the SC and HF groups, the HF and HO animals had reduced BMD and BMC (all $P < 0.001$). Four-week application of daily knee loading suppressed obesity and OVX induced reduction in BMD and BMC. After loading, a marked increase in the changes of BMD and BMC was observed (all $P < 0.001$; Fig. 4a and b).

Using H&E-stained sections, we further evaluated changes in bone loss by determining B.ar/T.ar and the circumference of trabecular bone (Fig. 4c and d). B.ar/T.ar in the HF and HO groups was significantly lower than that in the SC and HF groups, respectively ($P < 0.001$ in HF; $P < 0.05$ in HO). In response to knee-loading, B.ar/T.ar was increased in both obesity and OVX animals ($P < 0.001$ in HFL; $P < 0.05$ in HOL; Fig. 4e). Compared to animals in the SC and HF groups, the trabecular circumference in the HF and HO groups was significantly lower, respectively (both $P < 0.001$). However, the trabecular circumference in the loaded groups (HFL and HOL) was longer than that of the non-loaded groups (HF and HO) (both $P < 0.05$; Fig. 4f).

Knee loading promoted osteoblastic differentiation of BMSCs in obese mice

The effect of knee-loading on osteoblast was also determined. The number of osteoblasts, normalized with N.Ob/BS/mm, was significantly lower in the HF and HO groups than that in SC and HF, respectively (both $P < 0.001$). After knee-loading, the number of osteoblasts was increased (both $P < 0.01$; Fig. 5a and c).

ALP staining was employed to evaluate osteoblastic differentiation (Fig. 5b). In bone marrow-derived cells, the percentage of ALP-positive cells in the HF and HO groups was significantly lower than in the SC and HF groups, respectively (both $P < 0.001$). However, knee-loading increased the percentage of ALP-positive cells (both $P < 0.001$; Fig. 5d).

The involvement of Runx2 and ALP in osteoblast differentiation was examined (Fig. 5e). The levels of Runx2 and ALP in the HF group were significantly lower than in the SC group ($P < 0.001$, $P < 0.05$ respectively), and levels in the HO group were also lower than those in the HF group (both $P < 0.05$). After knee-loading, the loaded groups showed an increase in Runx2 and ALP expression levels compared to the non-loaded groups (all $P < 0.001$; Fig. 5f and g).

Knee loading regulated the expression of Wnt3a, LRP5, and β-catenin in obese mice

To assess the role of Wnt signaling in the knee-loading effect on adipocytes and osteoblasts differentiation, the expression of Wnt3a, LRP5, and β-catenin in the femur was examined. Immunohistochemistry analysis showed that a significant decrease in the number of Wnt3a-positive cells in HF was observed compared to SC ($P < 0.001$), and that in HO was also lower than that in the HF control group ($P < 0.001$). However, two loaded groups (HFL and HOL) presented higher numbers than the non-loaded groups (HF and HO), respectively (both $P < 0.001$; Fig. 6a and b). Western blotting indicated that a significant decrease in Wnt3a, LRP5, and β-catenin was observed in HF and HO compared to SC and HF, respectively ($P < 0.01$ in HF; $P < 0.05$ in HO). However, compared to the non-loaded groups, these levels were increased in the loaded groups (all $P < 0.01$; Fig. 6c-f).

The correlations between adipogenesis and osteogenesis in obese mice

To evaluate the effect of adipogenesis on bone loss, the correlations between adipogenesis and osteogenesis were analyzed. *In vivo*, A.ar/T.ar and the number of adipocytes were negative correlated with B.ar/T.ar and the number of osteoblasts (r= −0.827,−0.793, $P < 0.001$) (Fig. 7a and b). Body fat was negatively correlated with BMD (r= −0.837, $P < 0.001$) (Fig. 7c). *In vitro*, OD 250 for the differentiation of adipocytes was negatively correlated with ALP-positive osteoblasts differentiated from BMSCs (r= −0.85, $P < 0.001$) (Fig. 7d).

Discussion

This study presented that mechanical loading restrains obesity-associated bone loss by regulating the balance of cell fates between adipocytes and osteoblasts in obese mice, and Wnt3a signaling is involved in the loading effects. The results showed that the high-fat diet increased body weight, body fat, and body mass index, as well as bone loss than the standard diet, in which the changes in the combination of HF and OVX mice was even severer. Knee loading significantly decreased body weight, fat, and BMI. It also reduced the numbers and perimeter of adipocytes, the differentiation of adipocytes from BMSCs, and the levels of C/EBPα and PPARγ, Knee loading significantly suppressed OVX-induced reduction in BMD and bone mass. The loaded group also presented a significant increase in the number of osteoblasts on the trabecular surface, the levels of Runx2 and ALP, and the differentiation of BMSCs into osteoblasts. Furthermore, knee loading elevated the levels of Wnt3a, LRP5, and β-catenin. Collectively, the results indicate that knee loading can prevent obesity-related bone loss by altering the balance between adipocytes and osteoblasts via Wnt signaling (Fig. 7e).

Obesity and its associated metabolic sequelae are increasing worldwide. Its main cause includes high-calorie intake [34], lack of physical activity, and postmenopausal hormonal changes [35]. While obesity is a systemic metabolic disease, it is important to understand the underlying relationship between obesity and bone homeostasis. In humans, evidence indicates that elevated body mass is beneficial [36] and may improve bone quality at certain ages [37]. However, obese individuals have an elevated risk of bone

fracture, suggesting that in the longer-term, the presence of excessive adipose tissue may increase bone fragility [38]. This study used the high-fat diet and OVX to induce obese mice. The two obese groups (high-fat diet with or without OVX) presented high body weight, body fat, and BMI as well as bone loss, and the changes in OVX mice were even higher. Histological analysis showed that HFD-induced fat accumulation and bone loss are worse than those with OVX surgery. These results indicated that high-fat diet-induced obesity aggravates bone loss in OVX mice, consistent with the adverse effects of obesity on bone [39, 40]. The correlation analysis also showed that A.ar/T.ar, the number of adipocytes, and body fat is negatively correlated with B.ar/T.ar, the number of osteoblasts, and BMD, indicating the linkage of obesity to bone loss. Taken together, the present study indicates that the accumulation of excessive fats is associated with bone loss.

Understanding the effect of the marrow fat on bone metabolism is pivotal. Due to the accumulation of marrow adipose tissue [4], osteoporosis caused by obesity is characterized by an increase in marrow fat and a decrease in BMD in trabecular bone [41]. Regulating marrow adipocytes may be considered as a potential therapeutic target for osteoporosis [42]. The present study showed that knee loading reduced body weight, fat, BMI, the number, perimeter, and area ratio of adipocytes, while it elevated BMD, BMC, the circumference of trabecular bone, and the osteoblast number on the trabecular bone surface. An increase in adipose tissue in bone marrow could be associated with an imbalance of BMSCs differentiation [7], in which the differentiation into osteoblasts can alleviate bone loss [43]. The differentiation of bone marrow mesenchymal stem cells may be affected by varying transcription factors including PPARγ and RUNX2 necessary for adipogenesis and osteogenesis, respectively [44]. Herein, *in vitro* assays with bone marrow-derived cells showed that knee-loading inhibited differentiation into adipocytes by inhibiting C/EBPα and PPARγ and increased osteoblast differentiation by promoting Runx2 and ALP. There is a negative correlation between adipocytes and ALP-positive osteoblasts. The results indicated that regulating the balance between the differentiation of adipocytes and osteoblasts may contribute to preventing obesity-related bone loss.

Wnt/β-catenin signaling response to mechanical loading is critical for bone homeostasis [21, 45], and it is also reported to promote osteogenesis and inhibit adipogenesis [46]. Wnt/β-catenin signaling is a primary fate regulator of adipocytes and osteoblasts, whereby an accumulation of β-catenin was associated with a dose-dependent increase in osteogenesis and a decrease in adipocyte differentiation [47]. Our previous studies show that mechanical loading promotes bone remodeling by regulating osteoblasts and osteoclasts in the bone marrow through Wnt3a [19]. Immunohistochemistry and Western blotting in this study showed that knee loading increased the expression of Wnt3a, LRP5, and β-catenin. Wnt/β-catenin signaling might be involve in the differentiation of osteoblasts and adipocytes in response to knee loading.

Conclusions

In summary, this study demonstrates that knee loading is effective in decreasing body weight, fat, BMI, and increasing BMD, BMC, B.Ar/T.Ar in high-fat diet and OVX mice. Knee loading attenuates obesity-

linked bone loss by maintaining the balance of the adipocyte and osteoblast differentiation from BMSCs via Wnt signaling. The results are expected to provide a possibility of physical therapy such as mechanical loading for the treatment of obesity-associated bone loss. Further studies may focus on exploring the cell fate of osteoblast-adipocyte differentiation in bone marrow under mechanical loading.

Abbreviations

A.ar/T.ar, adipocyte area fraction (in %, T.ar = total tissue area, and A.ar = adipocytes area); ALP, alkaline phosphatase; B.ar/T.ar, bone trabecular area fraction (in %, T.ar = total tissue area, and B.ar = trabecular bone area); BMC, bone mineral content; BMD, bone mineral density; BMI, body mass index; BMSCs, bone marrow mesenchymal stem cells; C/EBPα, CCAAT/enhancer binding protein α; DAB, 3, 3'-diaminobenzidine; FBS, fetal bovine serum; H&E, hematoxylin and eosin; HFD, high-fat diet; LRP5, low-density lipoprotein receptor-related proteins 5; MAT, marrow adipose tissue; MEM-α, minimum essential medium α; MSCs, mesenchymal stem cells; N.Ob/BS, osteoblast number/bone surface; OVX, ovariectomy; pDEXA, peripheral dual-energy X-ray absorptiometry; PPARγ, peroxisome proliferator-activated receptor γ; Runx2, Runt-related transcription factor 2.

Declarations

Acknowledgements

Not applicable.

Funding

This work was supported by the grants from the National Natural Science Foundation of China (81772405, 81572100, and 81601863), Natural Science Foundation of Tianjin (18JCQNJC82200), and NIH (AR052144).

Competing Interest

All authors state that they have no conflict of interest.

Availability of data and materials

All supporting data are included in the article and its Additional files.

Ethics approval and consent to participate

All works involving animals were approved by the Ethics Committee of Tianjin Medical University.

Consent for publication

Not applicable.

Authors' contributions

Ping Zhang designed research; Xinle Li, Jie Li, Daquan Liu and Ping Zhang conducted research; Xinle Li, Jie Li, Keyu Wang, Hiroki Yokota and Ping Zhang analyzed the data; Xinle Li, and Ping Zhang wrote the manuscript. Ping Zhang approved the final manuscript as submitted. Ping Zhang accepted responsibility for integrity of data analysis.

References

1. Holman H, Dey S, Drobish I, Aquino L, Davis AT, Koehler TJ, et al. Obesity education in the family medicine clerkship: a US and Canadian survey of clerkship directors' beliefs, barriers, and curriculum content. BMC Med Educ. 2019;19(1):169.
2. Shapses SA, Pop LC, Wang Y. Obesity Is a Concern for Bone Health With Aging. Nutr Res. 2017;39:1-13.
3. Tencerova M, Kassem M. The bone marrow-derived stromal cells: Commitment and regulation of adipogenesis. Front Endocrinol (Lausanne). 2016;7:127.
4. Sebo ZL, Rendina-Ruedy E, Ables GP, Lindskog DM, Rodeheffer MS, Fazeli PK, et al. Bone marrow adiposity: basic and clinical implications. Endocr Rev. 2019;40(5):1187-1206.
5. Cuminetti V, Arranz L. Bone marrow adipocytes: the enigmatic components of the hematopoietic stem cell niche. J Clin Med. 2019;8(5):707.
6. Berendsen AD, Olsen BR. Osteoblast-adipocyte lineage plasticity in tissue development, maintenance and pathology. Cell Mol Life Sci. 2014;71(3):493–7.
7. Hu L, Yin C, Zhao F, Ali A, Ma J, Qian A. Mesenchymal stem cells: cell fate decision to osteoblast or adipocyte and application in osteoporosis treatment. Int J Mol Sci. 2018;19(2):360.
8. Yu C, Peall IW, Pham SH, Okolicsanyi RK, Griffiths LR, Haupt LM. Syndecan-1 Facilitates the Human Mesenchymal Stem Cell Osteo-Adipogenic Balance. Int J Mol Sci. 2020;21(11):3884.
9. Almalki SG, Agrawal DK. Key transcription factors in the differentiation of mesenchymal stem cells. Differentiation. 2016;92(1-2):41-51.
10. Maycas M, Esbrit P, Gortazar AR. Molecular mechanisms in bone mechanotransduction. Histol Histopathol. 2017;32(8):751-60. doi: 10.14670/HH-11-858.
11. Zhang P, Hamamura K, Yokota H, Malacinski GM. Potential applications of pulsating joint loading in sports medicine. Exerc Sport Sci Rev. 2009;37:52-56

12. Zhang P, Yokota H. Elbow loading promotes longitudinal bone growth of the ulna and the humerus. J Bone Miner Metab. 2012;30:31-39
13. Zhang P, Tanaka SM, Jiang H, Su M, Yokota H. Diaphyseal bone formation in murine tibiae in response to knee loading. J Appl Physiol. 2006;100:1452-59
14. Zhang P, Sun Q, Turner CH, Yokota H. Knee loading accelerates bone healing in mice. J Bone Miner Res. 2007;22:1979-87
15. Zhang P, Su M, Tanaka SM, Yokota H. Knee loading stimulates cortical bone formation in murine femurs. BMC Musculoskel Dis. 2006;7:73
16. Zhang P, Turner CH, Yokota H. Joint loading-driven bone formation and signaling pathways predicted from genome-wide expression profiles. Bone. 2009;44:989-98
17. Zhang P, Yokota H. Knee loading stimulates healing of mouse bone wounds in a femur neck. Bone. 2011;49:867-72
18. Liu DQ, Li XL, Li J, Yang J, Yokota H, Zhang P. Knee loading protects against osteonecrosis of the femoral head by enhancing vessel remodeling and bone healing. Bone. 2015;81:620-31
19. Li XL, Liu DQ, Li J, Yang S, Xu J, Yokota H, et al. Wnt3a involved in the mechanical loading on improvement of bone remodeling and angiogenesis in a postmenopausal osteoporosis mouse model. FASEB J. 2019;33(8):8913-24.
20. Tan N, Li XL, Zhai L, Liu DQ, Li J, Yokota H, et al. Effects of knee loading on obesity-related non-alcoholic fatty liver disease in an ovariectomized mouse model with high-fat diet. Hepatol Res. 2018;48(10):839-49.
21. Holguin N, Brodt MD, Silva MJ. Activation of Wnt signaling by mechanical loading is impaired in the bone of old mice, J Bone Miner Res. 2016;31(12):2215-26.
22. Grigorie D, Lerner UH. The crucial role of the Wnt system in bone remodelling, Acta Endocrinol (Buchar). 2018;14 (1):90-101.
23. Leucht P, Lee S, Yim N. Wnt signaling and bone regeneration: can't have one without the other, Biomaterials. 2019;196:46-50.
24. Chen X, Guo J, Yuan Y, Sun Z, Chen B, Tong X, et al. Cyclic compression stimulates osteoblast differentiation via activation of the Wnt/beta-catenin signaling pathway. Mol Med Rep. 2017;15 (5):2890-6.
25. Moseti D, Regassa A, Kim WK. Molecular regulation of adipogenesis and potential anti-adipogenic bioactive molecules. Int J Mol Sci. 2016;17(1):124.
26. Yuan Z, Li Q, Luo S, Liu Z, Luo D, Zhang B, et al. PPARγ and Wnt signaling in adipogenic and osteogenic differentiation of mesenchymal stem cells. Curr Stem Cell Res Ther. 2016;11(3);216-25.
27. Zhou J, Wang S, Qi Q, Yang X, Zhu E, Yuan H, et al. Nuclear factor I-C reciprocally regulates adipocyte and osteoblast differentiation via control of canonical Wnt signaling. FASEB J. 2017;31(5):1939-52.
28. Wu M, Wang Y, Shao J, Wang J, Chen W, Li Y. Cbfβ governs osteoblast–adipocyte lineage commitment through enhancing β-catenin signaling and suppressing adipogenesis gene expression.

Proc Natl Acad Sci U S A. 2017;114(38):10119-24.

29. Li J, Li XL, Liu D, Hamamura K, Wan Q, Na S, et al. eIF2α signaling regulates autophagy of osteoblasts and the development of osteoclasts in OVX mice. Cell Death Dis. 2019;10(12):921.
30. Krishnamoorthy D, Frechette DM, Adler BJ, Green DE, Chan ME, Rubin CT. Marrow adipogenesis and bone loss that parallels estrogen deficiency is slowed by low-intensity mechanical signals. Osteoporos Int. 2016;27(2):747-756.
31. Lee AM, Morrison JL, Botting KJ, Shandala T, Xian CJ. Effects of maternal hypoxia during pregnancy on bone development in offspring: a guinea pig model. Int J Endocrinol. 2014;2014:916918.
32. Yang S, Liu H, Zhu L, Li X, Liu D, Song X, et al. Ankle loading ameliorates bone loss from breast cancer–associated bone metastasis. FASEB J. 2019;33(10):10742-52.
33. Zheng W, Li X, Liu D, Li J, Yang S, Gao Z, et al. Mechanical loading mitigates osteoarthritis symptoms by regulating endoplasmic reticulum stress and autophagy. FASEB J. 2019;33 (3):4077-88.
34. Botchlett R, Woo SL, Liu M, Pei Y, Guo X, Li H, et al. Nutritional approaches for managing obesity-associated metabolic diseases. J Endocrinol. 2017;233(3):145-71.
35. Leeners B, Geary N, Tobler PN, Asarian L. Ovarian hormones and obesity, Hum Reprod Update. 2017;23(3):300-21.
36. Maimoun L, Mura T, Leprieur E, Avigon A, Mariano-Goulart D, Sultan A. Impact of obesity on bone mass throughout adult life: influence of gender and severity of obesity. Bone. 2016;90:23-30.
37. Kim HY, Jung HW, Hong H, Kim JH, Shin CH, Yang SW, et al. The role of overweight and obesity on bone health in Korean adolescents with a focus on lean and fat mass J Korean Med Sci. 2017;32 (10):1633-1641.
38. Palermo A, Tuccinardi D, Defeudis G, Watanabe M, D'Onofrio L, Lauria Pantano A, et al. Manfrini. BMI and BMD: the potential interplay between obesity and bone fragility. Int J Environ Res Public Health. 2016;13(6):544.
39. Hafner H, Chang E, Carlson Z, Zhu A, Varghese M, Clemente J, et al. Lactational high-fat diet exposure programs metabolic inflammation and bone marrow adiposity in male offspring. Nutrients. 2019;11(6):1393.
40. Jatkar A, Kurland IJ, Judex S. Diets high in fat or fructose differentially modulate bone health and lipid metabolism. Calcif Tissue Int. 2017;100(1):20-28.
41. Ilich JZ, Kelly OJ, Inglis JE. Osteosarcopenic obesity syndrome: what is it and how can it be identified and diagnosed? Curr Gerontol Geriatr Res. 2016;2016:7325973.
42. Singh L, Tyagi S, Myers D, Duque G. Good, bad, or ugly: the biological roles of bone marrow fat, Curr Osteoporos Rep. 2018;16(2):130-137.
43. Li CJ, Cheng P, Liang MK, Chen YS, Lu Q, Wang JY, et al. MicroRNA-188 regulates age-related switch between osteoblast and adipocyte differentiation. J Clin Invest. 2015;125(4):1509-22.
44. Meyer MB, Benkusky NA, Sen B, Rubin J, Pike JW. Epigenetic Plasticity Drives Adipogenic and Osteogenic Differentiation of Marrow-derived Mesenchymal Stem Cells. J Biol Chem.

2016;291(34):17829-47.
45. Bullock WA, Pavalko FM, Robling AG. Osteocytes and mechanical loading: The Wnt connection. Orthod Craniofac Res. 2019;22 Suppl 1:175-9.
46. Jing H, Su X, Gao B, Shuai Y, Chen J, Deng Z, et al. Epigenetic inhibition of Wnt pathway suppresses osteogenic differentiation of BMSCs during osteoporosis. Cell Death Dis. 2018;9(2):176.
47. Kim JA, Choi HK, Kim TM, Leem SH, Oh IH. Regulation of mesenchymal stromal cells through fine tuning of canonical Wnt signaling. Stem Cell Res. 2015;14(3):356-68.

Figures

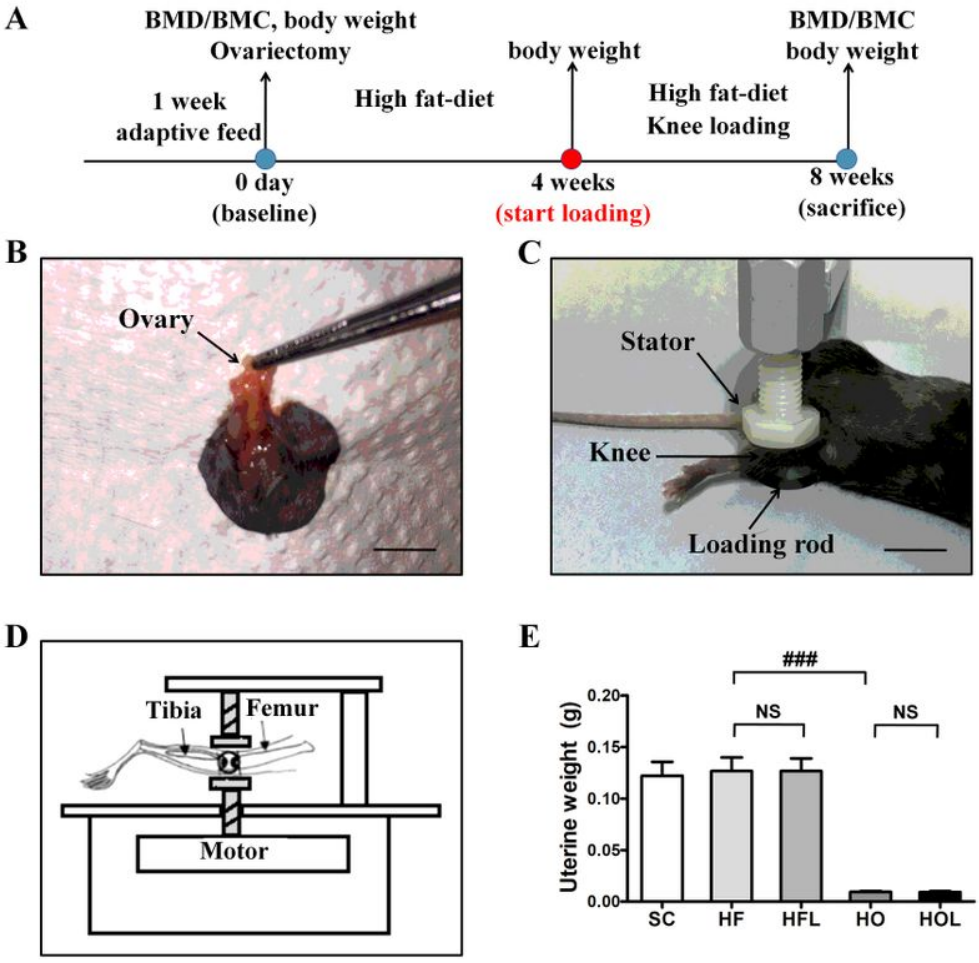

Figure 1

Experimental timeline, surgical diagram, and setting of knee loading. a After 1 week of acclimation, ovariectomy was carried out on HO and HOL. All mice except for SC were fed with the high-fat diet for 8 weeks, while SC was fed the standard chow diet. Knee loading was undertaken after 4 weeks of feeding with HFD. b Excision of bilateral ovaries to form estrogen-deficient obesity (Bar = 10 mm). c Loading was laterally applied to the left and right knee of mice successively (1 N, 5 Hz) with 6 min/day for 4 weeks (the loader was indicated by the arrow) (Bar = 10 mm). d Schematic diagram illustrated the loading

equipment. e Quantitative analysis of uterus mass (N = 10). The pound signs (###) represents statistical significance at P < 0.001.

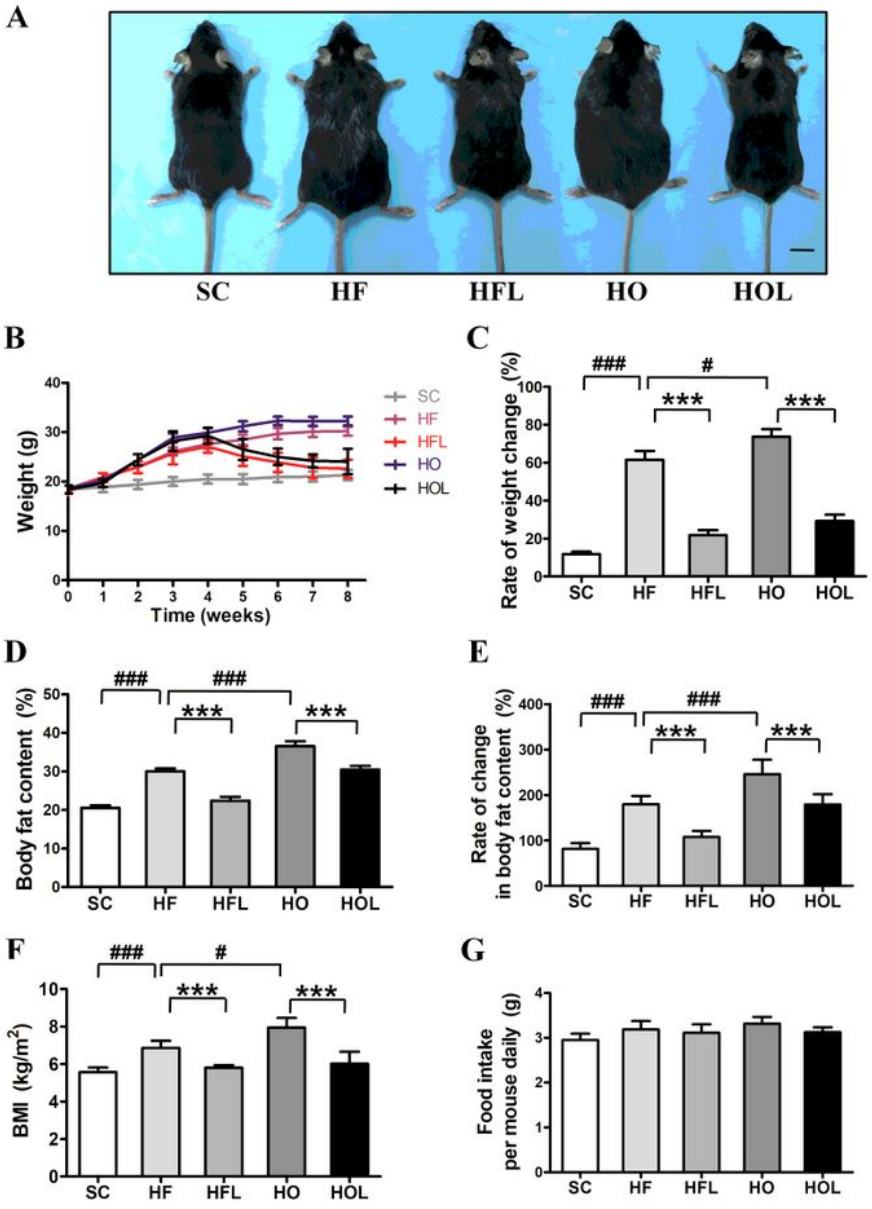

Figure 2

Reduction in body weight and fat mass in obese mice by knee loading. a Whole-body images in five groups (Bar = 10 mm). b Mean body weight. c Changes in body weight. d Whole-body fat content. e Changes in body fat content. f Body mass index. g Food intake per day among. The asterisks (* and ***)

represent statistical significance at P < 0.05 and P < 0.001, respectively. The pound signs (#, ## and ###) represent P < 0.05, P < 0.01, and P < 0.001, respectively (N = 15).

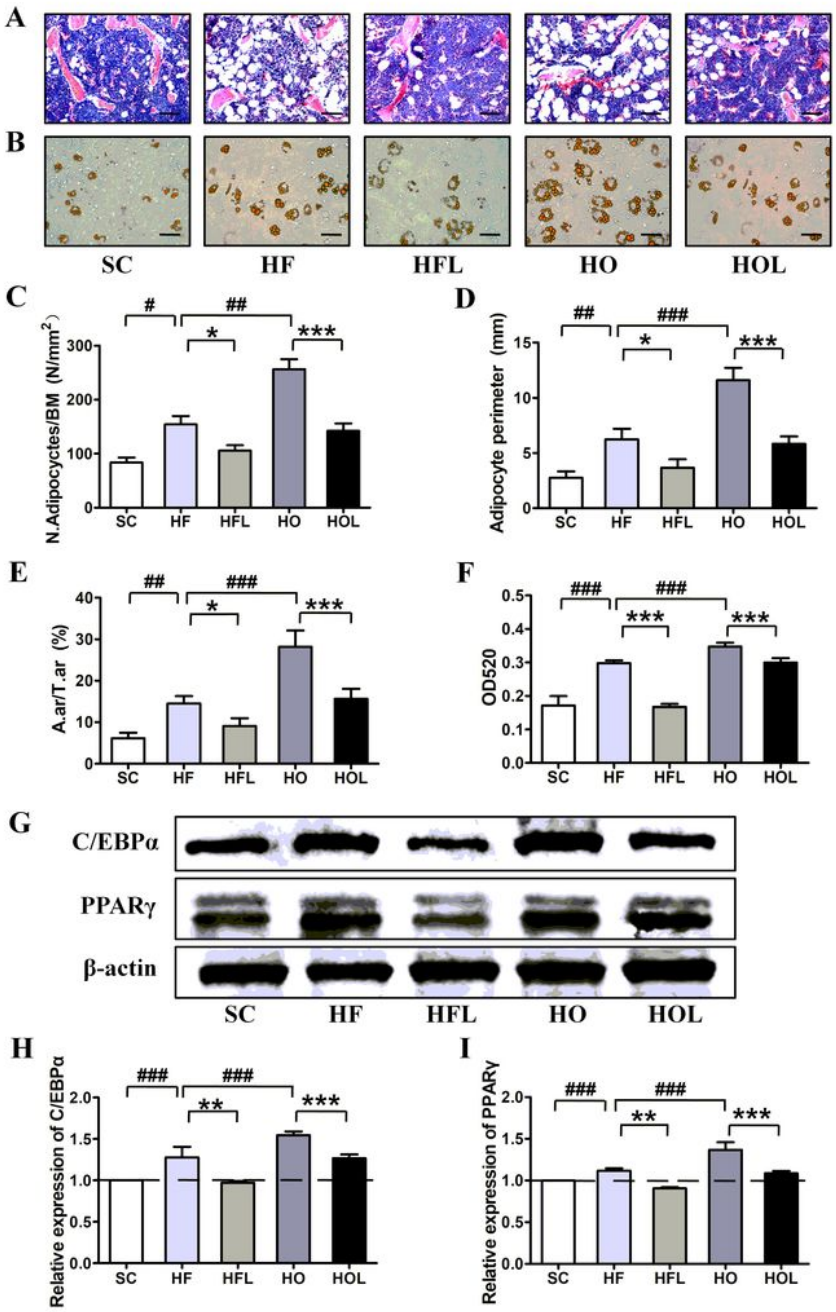

Figure 3

Inhibition in adipogenesis in vivo and in vitro by knee loading. a The histological parameters of the adipocyte in the femoral bone marrow cavity under the growth plate were determined by H&E staining (Bar = 100 μm). b Oil-red O staining was used to detect adipocyte differentiation (Bar = 50 μm). c-e

Measurement of marrow adipocyte number (c), perimeter (d) and A.ar/T.ar (e), respectively, in the distal femur region (N = 10). f Determination of oil red O-positive adipocytes by 520 nm absorbance analysis (N = 6). g-i Western blotting analysis of the adipogenic gene (C/EBPα, PPARγ) (g) and quantitative analysis of the relative intensity of C/EBPα (h) and PPARγ (i) (N = 6). The asterisks (*, **, and ***) represent statistical significance at P < 0.05, P < 0.01, and P < 0.001, respectively. The pound signs (#, ## and ###) represent P < 0.05, p < .01, and P < 0.001, respectively.

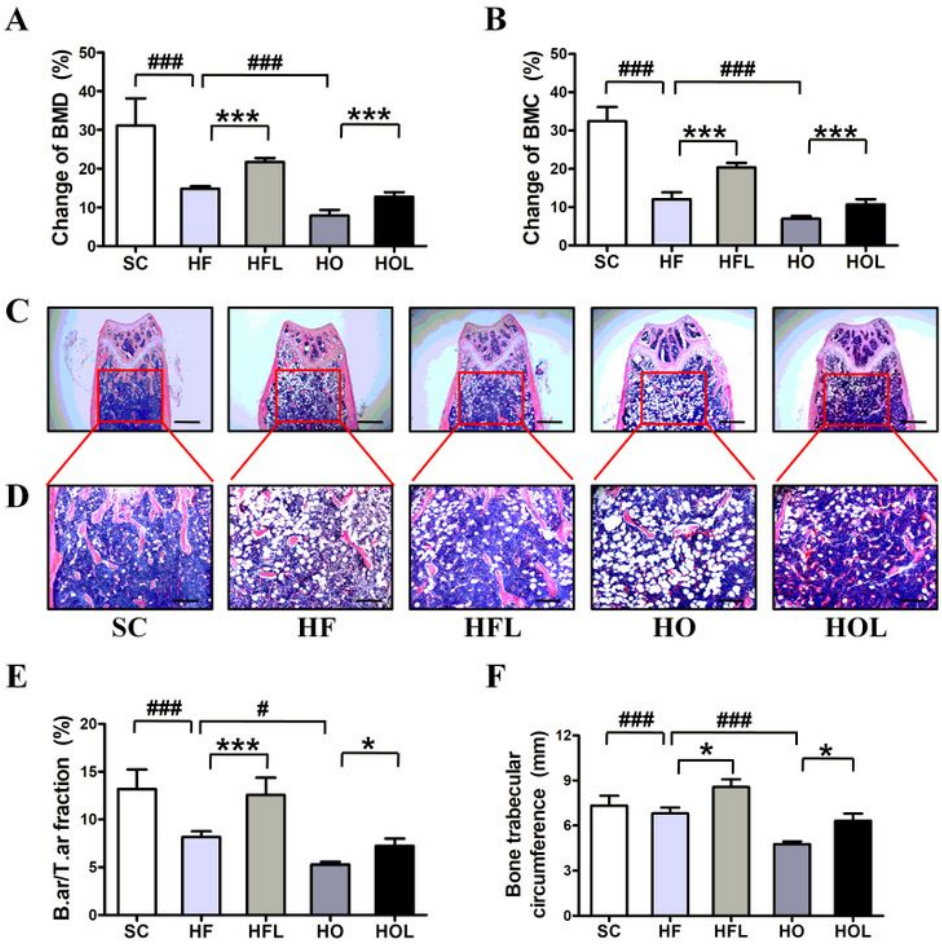

Figure 4

Reduction in bone loss in obese mice by knee loading in vivo. a-b BMD (a) and BMC (b) respectively, of the femurs, were measured on 0 day and 8 weeks, and their changes were determined. c-d The histological parameters of the trabecular bone in the femur under the growth plate were determined by H&E staining (Bar = 500 μm in C; Bar = 200 μm in D). e Measurement of B.ar/T.ar in the femur. f Measurement of the circumference of the trabecular bone. The asterisks (* and ***) represent statistical significance at $P < 0.05$ and $P < 0.001$, respectively. The pound signs (#, ## and ###) represent $P < 0.05$, $P < 0.01$, and $P < 0.001$, respectively (N = 10).

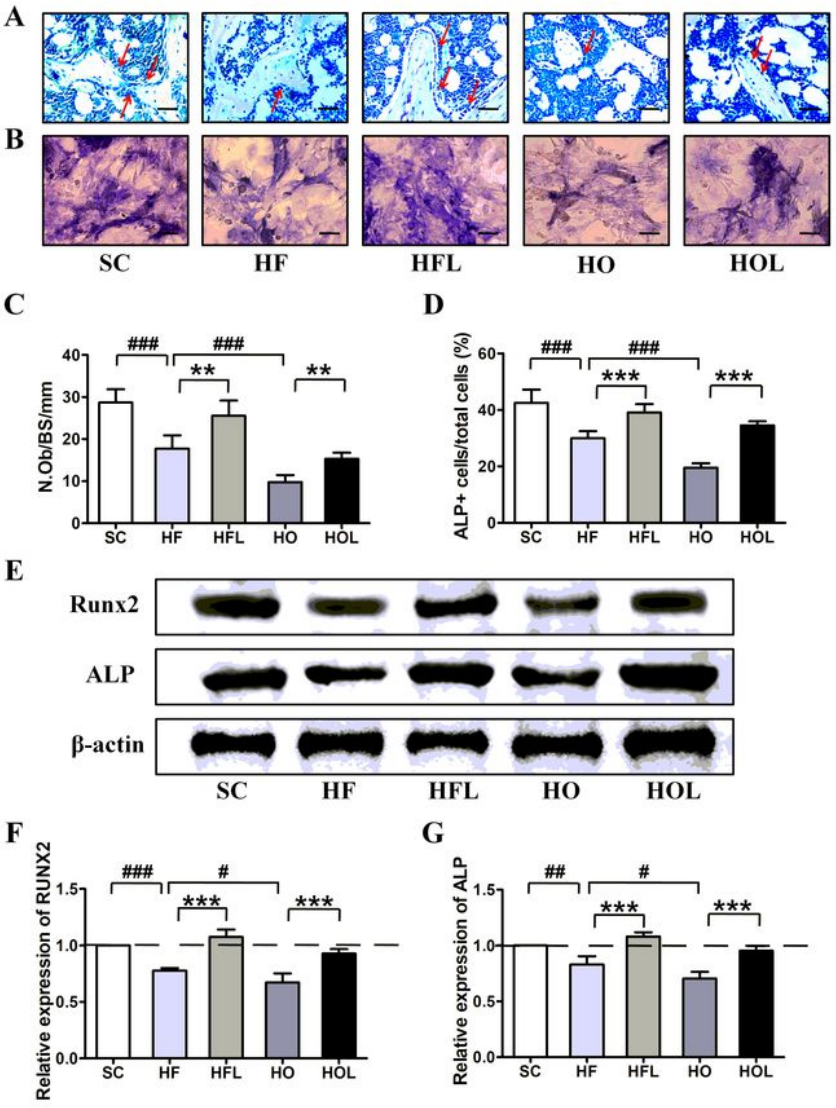

Figure 5

Promotion in osteogenesis in vivo and in vitro by knee loading. a MacNeal's staining was used to identify osteoblasts in the femur. Osteoblasts, located on the trabecular surface, were indicated by the arrows. (Bar = 50 μm). b Bone marrow-derived cells were cultured in 6-well plates for 14 days. ALP staining was used to detect osteoblast differentiation (Bar = 50 μm). c The representative photographs of the distal femur were used to evaluate the number of osteoblasts (N.Ob/BS/mm) (N = 10). d The ratio of the numbers of ALP-positive cells to that of total cells was determined (N = 6). e-g Western blotting analysis of the osteoblastogenic gene (Runx2, ALP) (e) and quantitative analysis of the relative intensity of Runx2 (f) and ALP (g) (N = 6). The asterisks (*, **, and ***) represent statistical significance at $P < 0.05$, $P < 0.01$, and $P < 0.001$, respectively. The pound signs (#, ## and ###) represent $P < 0.05$, $P < 0.01$, and $P < 0.001$, respectively.

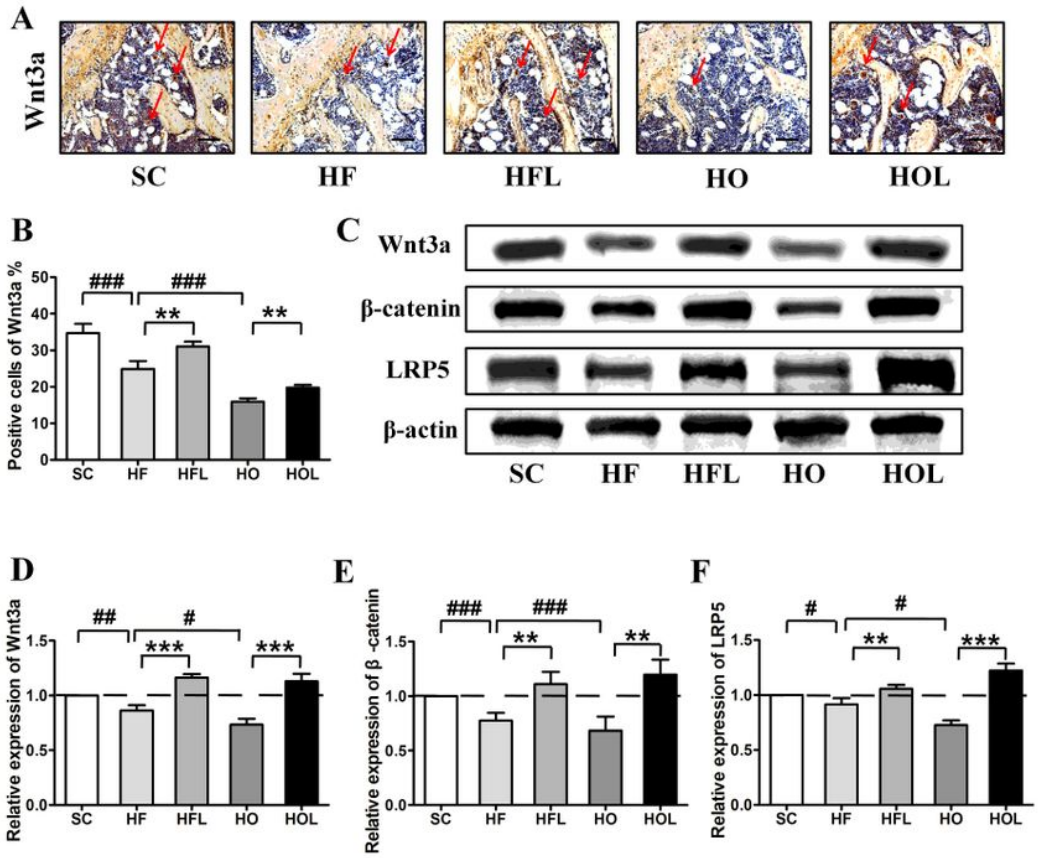

Figure 6

Activation of the Wnt/β-catenin pathway by knee loading in obese mice. a Immunohistochemistry staining of Wnt3a in the femur was conducted in vivo (Bar = 50 μm). The arrows indicated the positive cells. b The percentage of Wnt3a-positive cells was determined by immunohistochemistry in the distal femur (N = 10). c Representative images of Western blotting in the five groups for selected genes involved in the Wnt/β-catenin pathway (Wnt3a, LRP5, and β-catenin). d-f Quantified levels of relative intensity of Wnt3a (d), LRP5 (e), β-catenin (f) (N = 6). The asterisks (*, **, and ***) represent statistical significance at $P < 0.05$, $P < 0.01$, and $P < 0.001$, respectively. The pound signs (#, ## and ###) represent $P < 0.05$, $P < 0.01$, and $P < 0.001$, respectively.

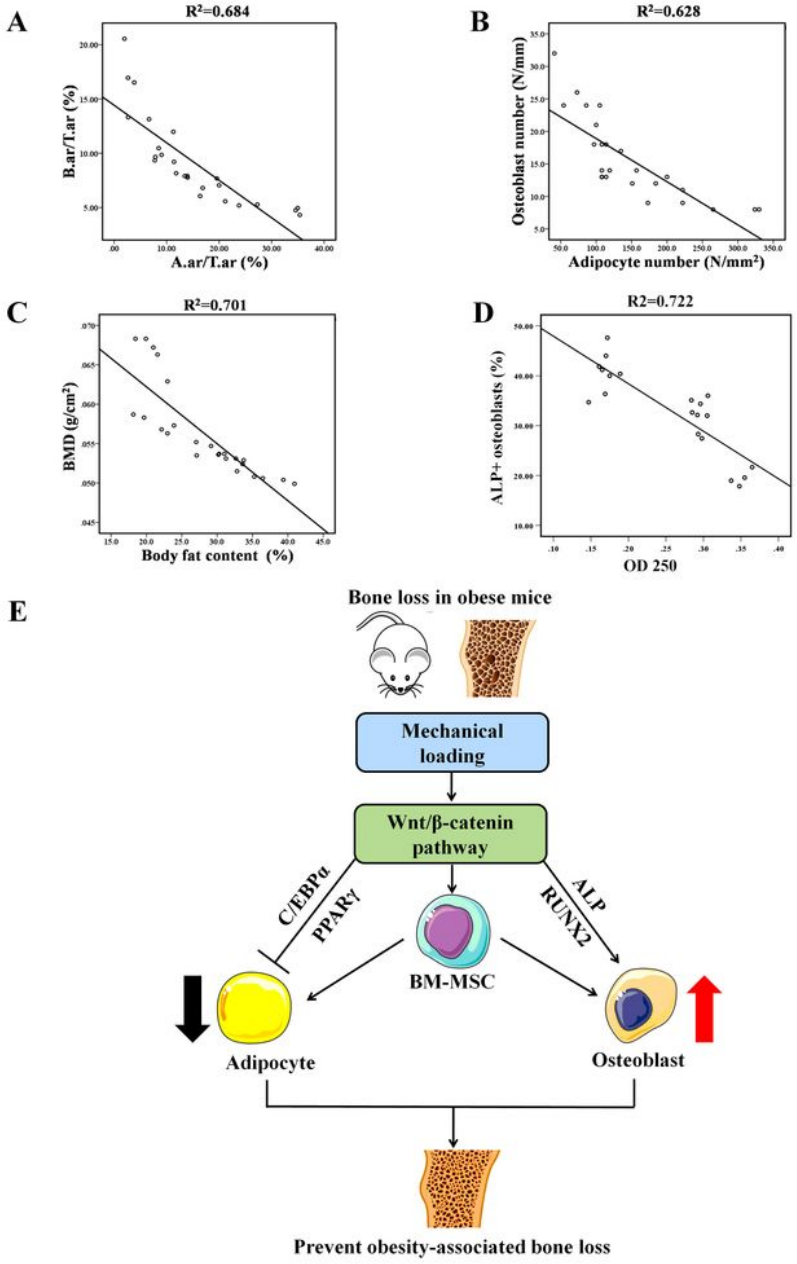

Figure 7

Correlation between parameters of adipocyte and osteoblast and proposed mechanism of knee loading. a Correlations between A.ar/T.ar and B.ar/T.ar. b Correlations between adipocyte number and osteoblast number. c Correlations between body fat and BMD. d Correlations between OD 250 for the differentiation of adipocytes and ALP-positive osteoblasts differentiated from BMSCs (N = 10). e Proposed mechanism of knee loading for obesity-associated bone loss.